Journal of Molecular Structure 1043 (2013) 103–108

Contents lists available at SciVerse ScienceDirect

Journal of Molecular Structure

journal homepage: www.elsevier.com/locate/molstruc

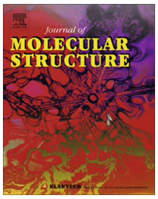

Synthesis, spectroscopic characterization and structural investigation of a new symmetrically trisubstituted benzene derivative: 3,3′,3″-(Benzene-1,3,5-triyl) tripropiolic acid

Alexander S. Münch [a], Felix Katzsch [b], Edwin Weber [b,*], Florian O.R.L. Mertens [a,*]

[a] Institute of Physical Chemistry, Technical University Bergakademie Freiberg, Leipziger Straße 29, 09596 Freiberg, Germany
[b] Institute of Organic Chemistry, Technical University Bergakademie Freiberg, Leipziger Straße 29, 09596 Freiberg, Germany

HIGHLIGHTS

- A new extended analogue of trimesic acid has been prepared.
- The structure of the compound is determined by single crystal X-ray diffraction.
- A new hydrogen bond motif of graph set $R_4^3(12)$ was obtained.

GRAPHICAL ABSTRACT

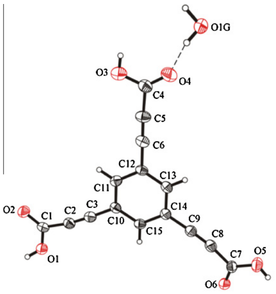

Crystal structure of 3,3′,3″-(Benzene-1,3,5-triyl)tripropiolic acid

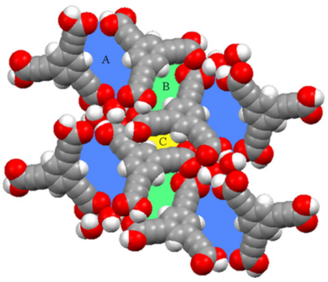

Packing structure with channel-like voids

ARTICLE INFO

Article history:
Received 28 February 2013
Received in revised form 3 April 2013
Accepted 3 April 2013
Available online 13 April 2013

Keywords:
1,3,5-Substituted benzene
Tripropiolic acid
Cross coupling reaction
Single crystal X-ray structure
Hydrogen bond interaction

ABSTRACT

The new 1,3,5-trisubstituted benzene derivative **1** featuring three propiolic acid side arms symmetrically attached to a benzene core has been synthesized. Spectroscopic studies including ^{1}H and ^{13}C NMR as well as FTIR measurements were performed. The single crystal structure of **1** shows involvement of a water molecule giving rise to formation of a new 12-membered hydrogen bonded ring motif of graph set $R_4^3(12)$ while the packing is typically interspersed with channel-like voids of different dimension containing additional ethanol and water molecules which, however, could not be localized precisely.

1. Introduction

Owing to their structural behavior, symmetrically trisubstitued benzenes have arisen interest for a long time [1] involving different fields of application such as discotic mesogens [2], amphiphiles [3] and gels [4], or organic electronic and optoelectronic materials [5]. Moreover, with the development of supramolecular chemistry, they have become particular relevant as construction elements for the design of trigonal tectons and other trigonally controlled framework components [6]. Aside from this, particular trisubstituted benzenes have also been used as chelating metal complexants, which include molecular capsules and containers, or to construct dendritic compounds as well as crystalline hosts and spacer-type building blocks for the formation of various aggregate structures [7]. Significant examples of these latter types of

---

* Corresponding authors. Tel.: +49 (0)3731 39 2386; fax: +49 (0)3731 39 3170 (E. Weber), tel.: +49 (0)3731 39 3192; fax: +49 (0)3731 39 3588 (F.O.R.L. Mertens).

E-mail addresses: edwin.weber@chemie.tu-freiberg.de (E. Weber), florian.mertens@chemie.tu-freiberg.de (F.O.R.L. Mertens).

0022-2860/$ - see front matter © 2013 Elsevier B.V. All rights reserved.
http://dx.doi.org/10.1016/j.molstruc.2013.04.005

aggregate structures are the organic–inorganic hybrid compounds, usually called metal–organic frameworks (MOFs) [8], the hydrogen bond stabilized networks (HNBs) [9], or the covalently linked organic frameworks (COFs) [10] as the latest development along this line of porous materials design. Within this frame, in particular symmetric tricarboxylic acids derived from benzene have proven very effective [11]. First and foremost, this is the case for the basic compound trimesic acid [12]. But also extended analogues that feature side arms with phenylene or ethynylene–phenylene spacer units inserted between the central ring and the carboxyl groups have been developed [13] though with the increasing length of the side arms, network interpenetration is becoming an increasing problem [14].

Remarkably, however, it seems that a more simply modified analogue of trimesic acid with only short alkyne moieties inserted between the aromatic core and the carboxyl groups **1** (Fig. 1), having the potential to reduce the tendency of network interpenetration, has neither been intended for MOF nor HBN formation. Related to this possibility, in the present paper we describe the synthesis of **1**, report results of spectroscopic studies, and discuss the single crystal structure of the new compound.

2. Experimental

2.1. General experimental and physical measurements

All denoted chemicals are commercially available and were used without further purification. Solvents (triethylamine and tetrahydrofuran) were subjected to standard drying procedures.

The melting points were measured on a microscope heating stage (Thermovar Reichert-Jung). ^{1}H and ^{13}C NMR spectra were recorded (25 °C) with a Bruker Avance III 500 NMR spectrometer at 500.13 MHz and 125.76 MHz, respectively, using $CDCl_3$ (**2**, **3**) and DMSO-d_6 (**1**) as solvent. Chemical shifts (δ) are given in ppm referring to tetramethylsilane as internal standard. The mass spectrum was measured on a Varian 3200Q-TRAP. The IR spectrum was obtained from a Varian 3100 FT-IR spectrometer in the region of 3800–450 cm^{-1} (KBr pellet). The TG–DSC analysis was performed with a Setaram Sensys TGA DSC coupled with the Varian TGA/IR interface under an argon flow of 20 mL/min in the temperature range from 25 to 500 °C using a temperature ramp of 5 K/min. The powder X-ray pattern was collected on a Philips X′Pert Diffractometer using Cu Kα radiation (λ = 1.541 Å, 40 kV, 30 mA). Scanning electron microscopy images were observed on a Jeol JSM 7001F scanning electron microscope using gold as a thin conducting layer.

2.2. Synthesis

2.2.1. 1,3,5-Tris(3-hydroxy-3-methyl-1-butynyl)benzene 3 [15]

1,3,5-Tribromobenzene (7.43 g, 23.59 mmol) was added to a mixture of 2-methylbut-3-yn-2-ol (MEBYNOL) (11.58 g, 184.12 mmol) and dry triethylamine (100 mL) under argon atmosphere. The stirred solution was degassed by heating for 1 h under argon. After cooling down the solution to room temperature, CuI (46 mg, 0.23 mmol) and $Pd(PPh_3)_4$ (400 mg, 0.6 mmol) were added. The resulting mixture was stirred at 25 °C for 30 min, then at 50 °C for 1 h and for 3.5 h under reflux. The solid was removed by filtration and washed with diethyl ether (2 × 30 mL). The combined organic solvents (filtrate and wash solution) were evaporated to give a dark colored solid. Crystallization from ethanol/water (1:1) yielded **3** as a pale gray powder (6.54 g, 86%). Mp = 169 °C. ^{1}H NMR (500.13 MHz, $CDCl_3$): δ_H = 7.39 (s, Ar—*H*), 1.59 (s, C*H*$_3$). ^{13}C NMR (125.76 MHz, $CDCl_3$): δ_C = 137.2, 123.3 (Ar—*C*), 94.9 (Ar—*C*≡C), 80.5 (Ar—C≡*C*), 65.5(*C*–$(CH_3)_2$OH), 31.4 (*C*H$_3$).

2.2.2. 1,3,5-Triethynylbenzene 2 [15]

A solution of **3** (6.54 g, 19.62 mmol) in toluene (100 mL) was heated up to boiling. Powdered potassium hydroxide (3.30 g, 58.86 mmol) was added and the mixture refluxed for 5 h. After cooling down to room temperature, diethyl ether (50 mL) was added. The organic phase was washed with water (2 × 100 mL), dried (Na_2SO_4), and evaporated to give a dark brown solid which was purified by sublimation at 80 °C under vacuum yielding colorless needles of **2** (1.56 g, 52%). Mp = 104 °C. ^{1}H NMR (500.13 MHz, $CDCl_3$): δ_H = 7.57 (s, Ar—*H*), 3.15 (s, C≡C—*H*). ^{13}C NMR (125.76 MHz, $CDCl_3$): δ_C = 135.6, 122.9 (Ar—*C*), 81.6 (Ar—*C*≡C), 78.7 (Ar—C≡*C*).

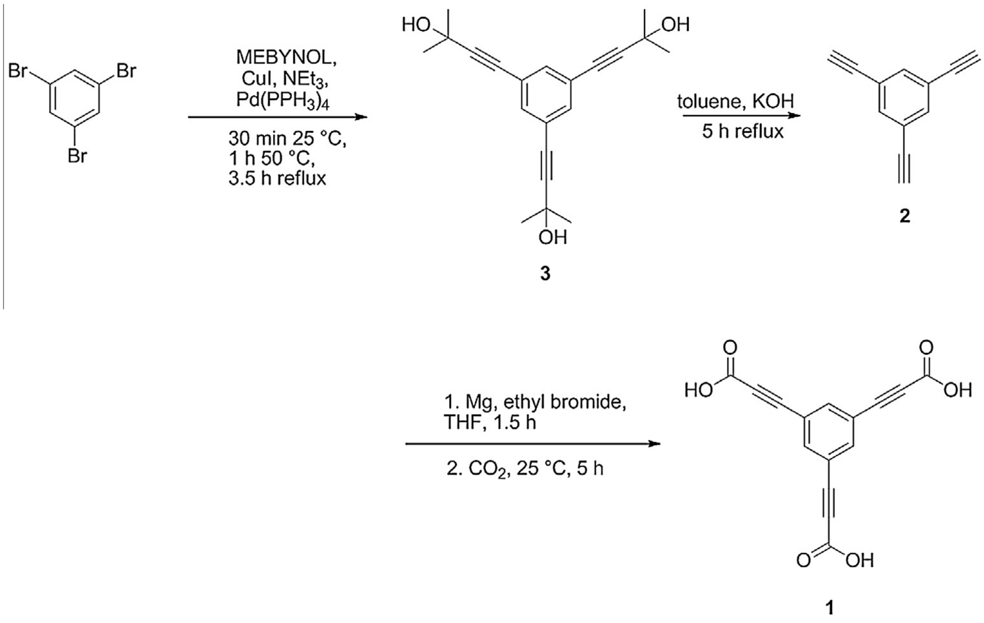

Fig. 1. Three step synthesis of compound **1**.

2.2.3. *3,3′,3″-(Benzene-1,3,5-triyl)tripropiolic acid* **1**

To a mixture of Mg (0.608 g, 25 mmol) in dry THF (25 mL), ethyl bromide (2.72 g, 25 mmol) in dry THF (10 mL) was added dropwise under an argon atmosphere. The mixture was stirred at room temperature until the formation of ethylmagnesium bromide was complete (1.5 h). Then, compound **2** (1.00 g, 6.70 mmol) in dry THF (10 mL) was added and the stirring was continued for 15 min. After that, CO_2 gas (99.2%, Praxair) was bubbled through the solution at room temperature for 5 h. During this time, a yellow brown solid was formed which changed the color to pale yellow. The reaction mixture was acidified with 5% aqueous hydrochloric acid (25 mL) and diluted with diethyl ether (25 mL) and water (25 mL). The organic phase was separated, washed with water (2×50 mL), dried (Na_2SO_4), and evaporated under reduced pressure. The residue was stirred in $CHCl_3$ (30 mL) at room temperature for 3 h, then collected, and dried in vacuum at 60 °C to yield **1** as a yellow powder (1.28 g, 68%). Mp 160 °C (dec.). ^{1}H NMR (500.13 MHz, DMSO-d_6): $\delta_H = 14.07$ (s, COO—*H*), 8.01 (s, Ar—*H*). ^{13}C NMR (125.76 MHz, DMSO-d_6): $\delta_C = 153.8$ (C—*C*OOH), 137.4 (Ar—*C*), 121.0 (Ar—*C*), 83.1 (Ar—*C*≡C), 81.0 (C≡*C*—COOH). IR: $\bar{\nu}$ = 3550, 3247, 3082, 2964, 2582, 2526, 2231, 1836, 1730, 1679, 1656, 1584, 1443, 1381, 1283, 1230, 1198, 1167, 1381, 913, 890, 795, 755, 672, 644, 607, 591. MS(ESI): *m*/*z* calc. for $C_{15}H_6O_6$: 282.02, found: 282.1 $[M]^+$.

2.3. *Single crystal X-ray analysis*

The single crystal X-ray diffraction data of compound **1** were collected at 100 K on a Bruker Kappa diffractometer equipped with an APEX II CCD area detector and graphite-monochromatized Mo Kα radiation ($\lambda = 0.71073$ Å) employing φ and ω scan modes. The data were corrected for Lorentz and polarization effects. Semiempirical absorption correction was applied using the SADABS program [16]. The SAINT program [16] was used for the integration of the diffraction profiles. The crystal structure was solved by direct methods using SHELXS-97 [17] and refined by full-matrix least-squares refinement against F^2 using SHELXL-97 [17]. All non-hydrogen atoms were refined anisotropically. The hydrogen atoms were generated at ideal geometrical positions and refined with the appropriate riding model. Geometrical calculations were performed using PLATON [18] and molecular graphics were generated using SHELXTL [17].

3. Results and discussion

3.1. *Synthesis of compound* **1**

For the synthesis of compound **1**, a three-step reaction sequence as specified in Fig. 1 was used. In the first step, this involves reaction of 1,3,5-tribromobenzene with 2-methylbut-3-yn-2-ol applying a Pd-catalyzed Sonogashira–Hagihara C—C coupling protocol [19,20] to the protected trialkyne **3**. In a second step, the protecting groups at the alkyne side arms were removed by treatment with potassium hydroxide to give **2**. Following a related procedure [21] in the closing step, **2** was converted to **1** via a Grignard addition to carbon dioxide with the Grignard reagent being derived from **2** and ethylmagnesium bromide (prepared from ethyl bromide and magnesium). Considering the sequence of reactions, **1** has been obtained in an overall yield of 30%.

All synthesized compounds were confirmed by melting point measurements and ^{1}H and ^{13}C NMR spectroscopy. In addition, the target compound **1** was characterized by IR spectroscopy, mass spectrometry, and TG–DSC measurement.

3.2. *FTIR spectroscopic study of* **1**

The FTIR spectrum of **1** was recorded in the region from 450 to 3800 cm^{-1} using a KBr pellet. Fig. 2 demonstrates the corresponding IR spectrum of a crystalline sample dried in vacuum at 60 °C for 3 h which does not indicate any typical bands of the solvents mesitylene and ethanol that have been used for crystallization. However, an intensive and broad band at 3247 cm^{-1} denotes the inclusion of water molecules in the lattice. This result points to the fact that strong hydrogen bonding between the carboxyl groups and water molecules may have formed.

Moreover, specific bands of the organic acid function can be determined, such as O—H stretches at 2964 cm^{-1}, overtone and combination bands in the range between 2526 and 2600 cm^{-1}, C═O stretch mode at 1730 cm^{-1}, in plane O—H band at

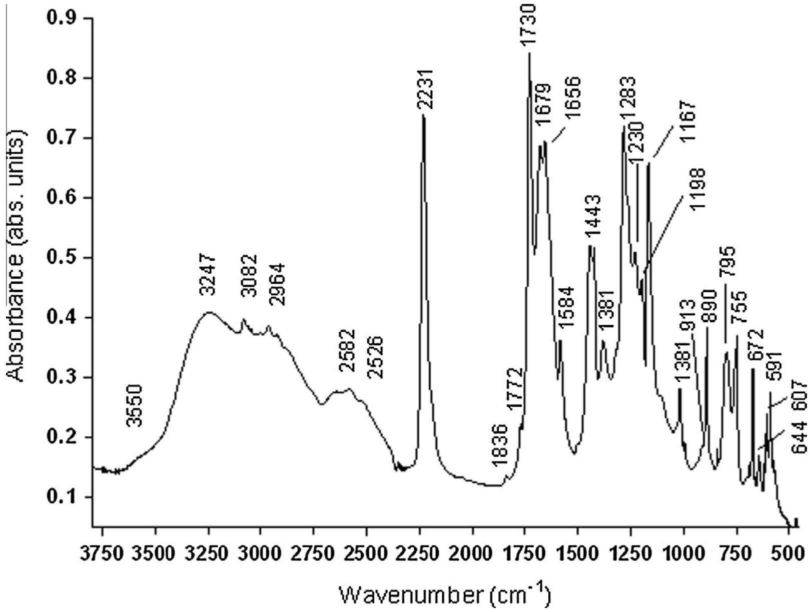

Fig. 2. FTIR spectrum of **1** between 3800 and 450 cm^{-1} (KBr pellet).

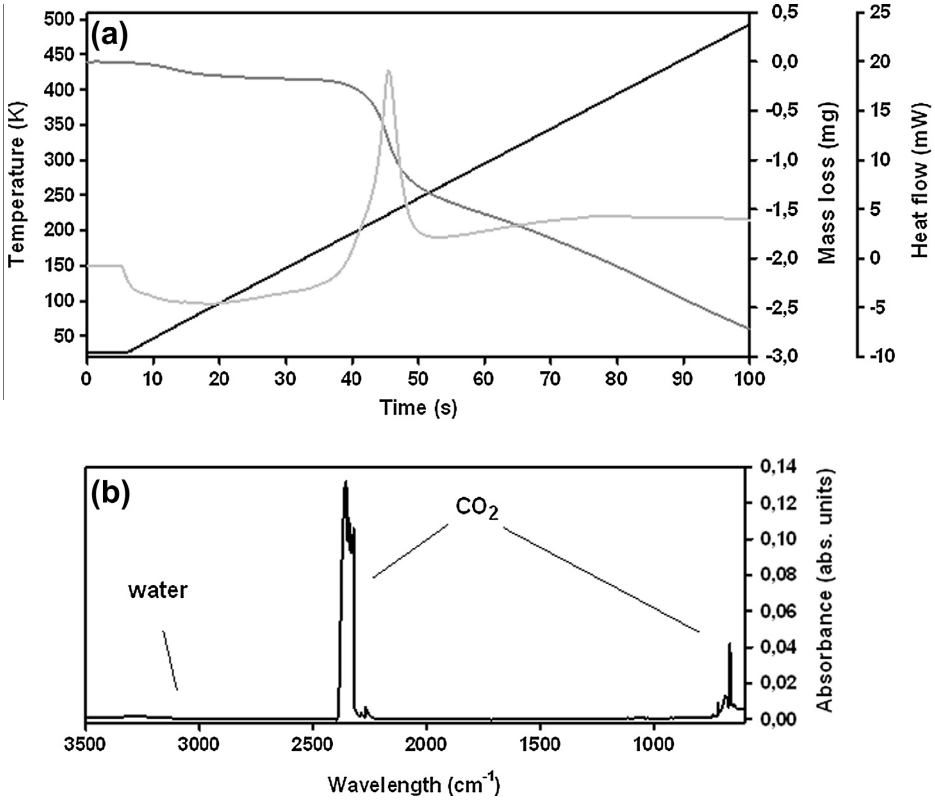

Fig. 3. TG–DSC analysis (a) of **1** combined with the IR spectrum of the gases released from the heated sample after 40 min (b). Curves in the upper diagram: black – temperature ramp, gray – mass flow, and light gray – heat flow.

1422 cm^{-1}, C—O vibration at 1283 cm^{-1}, and an out-of-plane O—H band at 913 cm^{-1}. The intensive IR mode at 2231 cm^{-1} indicates the characteristic C≡C stretch band of a disubstituted alkyne. Beside these vibration bands, typical modes of the aromatic ring are found, including C—H stretches between 3000 and 3100 cm^{-1}, summation bands at 1772 and 1836 cm^{-1}, ring modes at 1443 and 1584 cm^{-1}, an in-of-plane C—H vibration at 1167 cm^{-1}, and an out-of-plane C—H band at 890 cm^{-1}. The vibration modes at 672, 890, and 1584 cm^{-1} are bands characteristic of the 1,3,5-substitution pattern of the aromatic ring [22].

3.3. TG–DSC analysis of 1 coupled with IR spectroscopy

The thermogravimetry coupled with differential scanning calorimetry of 5.35 mg of **1** were performed under an argon flow of 20 mL/min in the temperature range from 25 to 500 °C (Fig. 3a). In order to investigate gases released by heating effects like decomposition, the TG-DSC setup was coupled with an IR spectrometer. At first, a sample of single crystals was intensively dried in vacuum at 100 °C for 5 h removing all solvent molecules, like water, ethanol, or mesitylene. The obtained TG curve possesses only one step beginning at 160 °C. After 40 min, the corresponding IR spectrum shows a flat broad band at 3250 cm^{-1} typical of the O—H stretch vibrations of water, two high bands at 2320 and 2355 cm^{-1} correlating with an asymmetric C=O valence vibration of carbon dioxide, and a band at 667 cm^{-1} belonging to the deformation vibration of CO_2. In addition, an exothermic effect was observed which is unusual for melting processes (Fig. 3a). Thus, it can be reasoned that the synthesized tricarboxylic acid decomposes at a temperature higher than 160 °C. The evaluation of the peak area results in a value of −233 kJ/mol for the decomposition enthalpy.

Table 1
Crystal data and refinement details of the structure determination.

Crystal data	**1**
Empirical formula	$C_{15}H_6O_6{\cdot}H_2O$
Formula weight (g/mol)	300.21
Crystal description	Yellow needle
Crystal system	Monoclinic
Space group	$P2_1/n$
Unit cell dimension (Å)	a = 13.9613(7) b = 3.7082(2) c = 30.6316(17) β = 92.505(4)
V (Å^3)	1584.32(15)
Z	4
Dx (g cm^{-3})	1.259
Absorption coefficient (mm^{-1})	0.102
F(000)	616
Crystal size (mm)	0.53 × 0.15 × 0.05
Data collection	
Temperature (K)	100(2)
Radiation, wavelength (Å)	Mo Kα, 0.71073
Collected reflections	20,949
θ Range (°)	1.33–25
Index ranges ±h ±k ±l	−16/16, −4/4, −36/36
Unique data, R_{int}	2808, 0.0595
R_1, wR_2 [$I > 2\sigma(I)$]	0.0507, 0.1318
R_1, wR_2 (all data)	0.0753, 0.1451
Refinement	
N_{ref}, N_{par}	2808, 209
Goodness of fit on F^2	1.06
Max. and av. shift/error	0.000, 0.000
Min. and max. resid. dens. (e Å^3)	−0.218, 0.419

3.4. X-ray single crystal analysis of 1

Slow evaporation of the solvent from a solution of **1** in mesitylene/ethanol/water (10:1:1) yielded transparent yellow needles

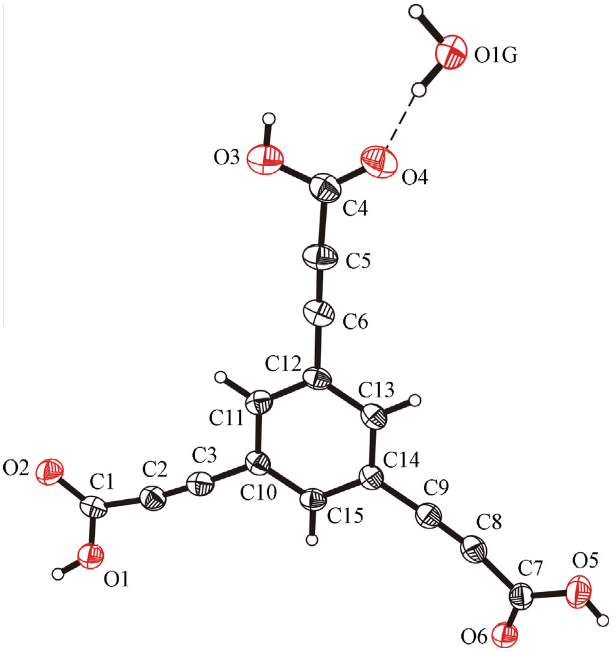

Fig. 4. Molecular structure of **1**, showing the atom labeling scheme with displacement ellipsoids drawn at the 50% probability level.

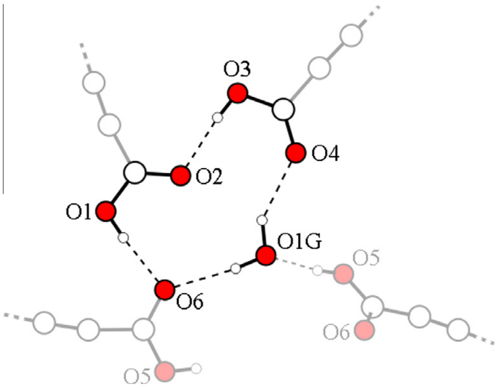

Fig. 5. Hydrogen bond motif $R_4^3(12)$ including numbering of the involved oxygen donor and acceptor atoms.

Table 2
Selected intermolecular hydrogen bonds of the studied structure.

Atoms involved	Symmetry	Distance (Å)		Angle (°)
		D···A	H···A	D–H···A
O1–H1···O6	2 – *x*, 3 – *y*, –*z*	2.617(2)	1.78	171
O3–H3···O2	1 – *x*, 1 – *y*, –*z*	2.676(2)	1.84	172
O5–H5···O1G	1 + *x*, 1 + *y*, *z*	2.490(2)	1.66	172
O1G–H1G···O6	3/2 – *x*, –3/2 + *y*, 1/2 – *z*	2.922(3)	1.99	162
O1G–H2G···O4	1/2 – *x*, 1/2 + *y*, 1/2 – *z*	2.870(3)	2.00	148

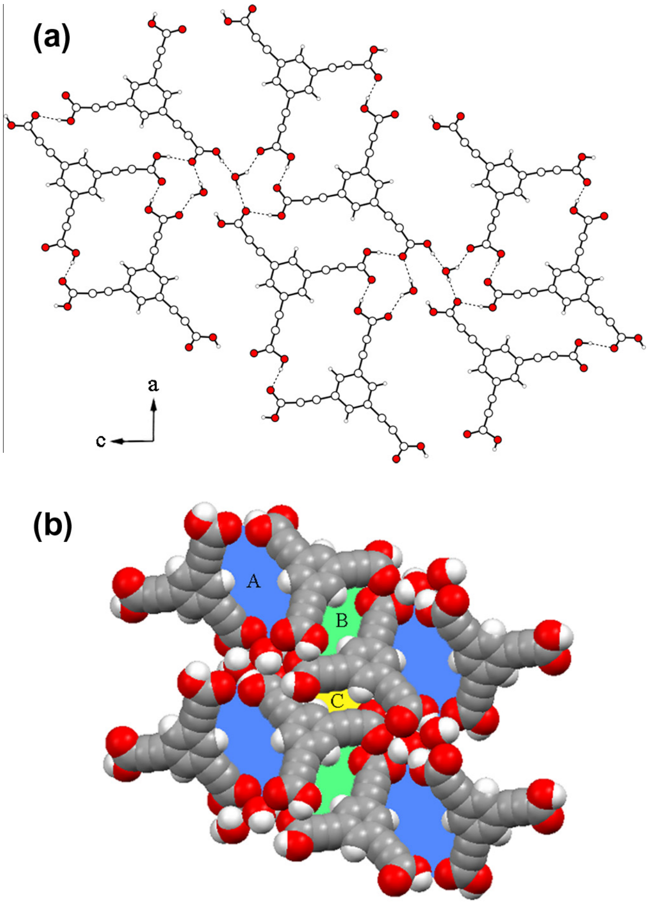

Fig. 6. Packing structure of **1** (a) and van-der-Waals model including illustration of the channel framework (b).

suitable for single crystal X-ray investigation. Crystal data and details of the structure determination are given in Table 1. The compound crystallizes in the monoclinic space group $P2_1/n$, with the unit cell containing **1**, water and ethanol. While the water molecules are integrated in the crystal lattice by connecting the carboxyl functions, the other solvent molecules are only included in the porous host lattice. Although the measurement took place at 100 K, it was not possible to precisely localize and refine the only weakly bonded or disordered guest molecules. Therefore, the high residual electron density was removed by the SQUEEZE method of the PLATON program [18] and corresponds to approximate two ethanol and two water molecules per unit cell. The further refinement was executed with the solvent free host structure.

The molecular structure of the compound in the crystal is presented in Fig. 4 showing that the ethynyl substituents deviate from the ideal linear geometry, which is obvious considering the alkyne bond angles [171.97° (C1–C2–C3) and 177.21° (C2–C3–C10); 176.77° (C4–C5–C6) and 179.64° (C5–C6–C12); 170.93° (C7–C8–C9) and 176.31° (C8–C9–C14)]. This deviation is probably a consequence of the molecular arrangement in the solid state and the intermolecular interactions being effective [23]. Furthermore, the carboxyl groups are slight twisted with respect to the aromatic ring plane as indicated by the interplanar angles of 9.08° (O1–C1–O2), 6.66° (O3–C4–O4) and 13.66° (O5–C7–O6). In contrast to the hydrogen bonded “chicken-wire” network typical for trimesic acid [24], the structure of **1** shows a distinct difference in so far that a water molecule is involved giving rise to a particular network pattern. More strictly speaking, a water molecule as hydrogen bond donor connects two carbonyl functions of two different molecules of **1** by strong O—H···O bonds [d(O1G···O4) = 2.870(3) and d(O1G···O6) = 2.922(3) Å] [25,26]. A carboxyl group of another molecule of **1** is included via hydrogen bonding [d(O3···O2) = 2.676(2) and d(O1···O6) = 2.617(2) Å] to yield a new ring motif which follows the graph set $R_4^3(12)$ (Fig. 5). Parameter details of the hydrogen bonding interactions are specified in Table 2.

In the crystal packing, the molecules form a tape structure with superimposed tapes held together by π–π interactions between the aromatic rings [27] and the alkyne units [28]. Tapes which lie side by side are twisted against each other (interplanar angle: 60.63°) and are stabilized by strong O—H···O bonds [d(O5···O1G) = 2.490(2) Å] between the acid hydroxyl group O5–H5 and the water oxygen O1G. Three different types of channel-like voids (A, B and C) exist in the lattice having different dimensions (Fig. 6). Ethanol is probably included in the biggest channel (A, ca. 4.0 × 6.1 Å^2), whereas water should be included in the smaller channel (B, ca. 2.3 × 3.1 Å^2). The third channel (C, 1.7 × 2.4 Å^2) is most probably unfilled because it is too small for inclusion of any solvent molecules. With the PLATON program [18], a packing index of the unit cell of 60.5% and a solvent accessible void of 321.3 Å^3, which equates to 20% of the unit cell volume, was calculated.

4. Conclusion

A new trigonal compound **1** featuring three propiolic acid side arms symmetrically attached to a benzene core, being expected to be a useful building block in the design and construction of metal–organic or hydrogen bond stabilized networks, has been synthesized via a three step reaction sequence involving metal assisted coupling procedures. ^{1}H and ^{13}C NMR as well as FTIR spectroscopic data show characteristic properties of the compound constitution. TG–DSC analysis combined with IR measurements demonstrate instability of **1** exposed to a temperature higher than 160 °C by the escape of carbon dioxide. In the crystalline state, **1** is involved in hydrogen bonding to water molecules, giving rise to a new hydrogen-bonded ring motif following the graph set $R_4^3(12)$. The packing structure is typically interspersed with channel-like voids (A, B and C) of different dimensions containing proportional to their sizes additional solvent molecules, i.e. ethanol (A) or water (B). These interstitially included solvent molecules obviously contribute to the stability of the crystal lattice since a distinct change or decay of the crystal structure is indicated upon their removal. Nevertheless, the presented linker- or tecton-type molecule **1** could be useful for the formation of porous metal–organic frameworks helping to suppress interpenetration because of its moderate length and rigidity of the side arms. Aside, the ethynylic π-electrons could interact with small molecules in ways that can be exploited for the practical use of the respective compounds.

Acknowledgments

Financial support by the European Union (European regional development fund) and by the Ministry of Science and Art of Saxony (Cluster of Excellence "Structure Design of Novel High-Performance Materials via Atomic Design and Defect Engineering [ADDE]") is gratefully acknowledged by F.K. A.M. thanks the Deutsche Forschungsgemeinschaft (Priority Program 1362 "Porous Metal-Organic Frameworks") for financial support. We thank Anja Obst for conducting the SEM measurements, Jürgen Seidel and Jutta Lange for carrying out the TG–DSC–IR measurements.

Appendix A. Supplementary material

The crystallographic information file has been deposited by using the Cambridge structure database (CCDC 912744). These data can be obtained free of charge via www.ccdc.cam.ac.uk/data-request/cif, by e-mailing data-request@ccdc.com.ac.uk or by contacting the Cambridge CB21 EZ, UK; fax: +44 1223 336033. Supplementary data associated with this article can be found, in the online version, at http://dx.doi.org/10.1016/j.molstruc.2013.04.005.

References

[1] D.B. Clapp, A.A. Morton, J. Am. Chem. Soc. 58 (1936) 2172.

[2] (a) S. Chandrasekhar, G.A. Ranganath, Rep. Prog. Phys. 53 (1990) 57;
(b) S. Sergeyev, W. Pisula, Y.H. Geerts, Chem. Soc. Rev. 36 (2007) 1902;
(c) R.J. Bushby, K. Kawata, Liq. Cryst. 38 (2011) 1415.

[3] (a) P. Besenius, K.P. van den Hout, H.M.H.G. Albers, T.F.A. de Greef, L.L.C. Olijve, T.M. Hermans, B.F.M. de Waal, P.H.H. Bomans, N.A.J.M. Sommerdijk, G. Portale, A.R.A. Palmans, M.H.P. van Genderen, J.A.J.M. Vekemans, E.W. Meijer, Chem. Eur. J. 17 (2011) 5193;
(b) E. Weber, Angew. Chem. Int. Ed. 22 (1983) 616.

[4] D.K. Smith, in: J.L. Atwood, J.W. Steed (Eds.), Organic Nanostructures, Wiley-VCH, Weinheim, 2008, pp. 111–154.

[5] (a) K. Nøgaard, M.B. Nielsen, T. Bjørnholm, in: T.J.J. Müller, U.H.F. Bunz (Eds.), Functional Organic Materials, Wiley-VCH, Weinheim, 2007, pp. 353–392;
(b)B. Pignataro (Ed.), Molecules at Work, Wiley-VCH, Weinheim, 2012.

[6] (a) J.W Steed, D.R Turner, K.J Wallace, Core Concepts in Supramolecular Chemistry and Nanochemistry, Wiley, Chichester, 2007;
(b) J.W. Steed, A.L. Atwood, Supramolecular Chemistry, second ed., Wiley, Chichester, 2009.

[7] (a) F. Vögtle, G. Richard, N. Werner, Dendrimer Chemistry, Wiley-VCH, Weinheim, 2009;
(b) D.D. MacNicol, G.A. Downing, in: D.D. MacNicol, F. Toda, R. Bishop (Eds.), Comprehensive Supramolecular Chemistry, vol. 6, Elsevier, Oxford, 1996, pp. 421–464;
(c) F. Vögtle, E. Weber, Angew. Chem. Int. Ed. 18 (1979) 753.

[8] (a)K. Rurack, R. Martínez-Máũez (Eds.), The Supramolecular Chemistry of Organic–Inorganic Hybrid Materials, Wiley, Hoboken, 2010;
(b)L.R. MacGillivary (Ed.), Metal-Organic Frameworks, Wiley, Hoboken, 2010;
(c) A.S. Münch, J. Seidel, A. Obst, E. Weber, F.O.R.L. Mertens, Chem. Eur. J. 17 (2011) 10958.

[9] (a) J.A.A.W. Elemans, S. Lei, S. De Feyter, Angew. Chem. Int. Ed. 48 (2009) 7298;
(b) D. Bonifazi, S. Mohnani, A. Llanes-Pallas, Chem. Eur. J. 15 (2009) 7004.

[10] (a) J.-X. Jiang, F. Su, A. Trewin, C.D. Wood, N.L. Campbell, H. Niu, C. Dickinson, A.J. Ganin, M.J. Rosseinsky, Y.Z. Khimyak, A.I. Cooper, Angew. Chem. Int. Ed. 46 (2007) 8574;
(b) E. Sheepwash, V. Krampe, R. Scopelliti, O. Sereda, A. Neels, K. Severin, Angew. Chem. Int. Ed. 50 (2011) 3034.

[11] (a) D. Kim, X. Song, J.H. Yoon, M.S. Lah, Cryst. Growth Des. 12 (2012) 4186;
(b) J. Li, Z. Ma, K. Deng, S. Lei, Q. Zeng, X. Fan, S. De Feyter, W. Huang, C. Wang, Chem. Eur. J. 15 (2009) 5418;
(c) S. Förster, W. Seichter, E. Weber, Z. Naturforsch. 66b (2011) 939.

[12] (a) G. Férey, C. Serre, C. Mellot-Draznieks, F. Millange, S. Surblé, J. Dutour, I. Margiolaki, Angew. Chem. Int. Ed. 43 (2004) 6296;
(b) C. Mellot-Draznieks, J. Dutour, G. Férey, Angew. Chem. Int. Ed. 43 (2004) 6290;
(c) S. Griessl, M. Lackinger, M. Edelwirth, M. Hietschold, W.M. Heckl, Single Mol. 3 (2002) 25;
(d) A. Dimitriev, N. Lin, J. Weckesser, J.V. Barth, K. Kern, J. Phys. Chem. B 106 (2002) 6907;
(e) S.V. Kolotuchin, E.E. Fenlon, S.R. Wilson, C.J. Loweth, S.C. Zimmerman, Angew. Chem. Int. Ed. 34 (1995) 2654.

[13] L. Kampschulte, M. Lackinger, A.-K. Maier, R.S.K. Kishore, S. Griessl, M. Schnittel, W.M. Heckl, J. Phys. Chem. B 110 (2006) 10829.

[14] (a) P. Vishweshwar, D.A. Beauchamp, M.J. Zaworotko, Cryst. Growth Des. 6 (2006) 2429;
(b) B.R. Bhogala, P. Vishweshwar, A. Nangia, Cryst. Growth Des. 2 (2002) 325.

[15] W. Shu, C. Guan, W. Guo, C. Wang, Y. Shen, J. Mater. Chem. 22 (2012) 3075.

[16] S.A.I.N.T. Bruker, SADABS, Bruker AXS Inc., Madison, Wisconsin, USA, 2007.

[17] G.M. Sheldrick, Acta Crystallogr. A64 (2008) 112.

[18] A.L. Spek, Acta Crystallogr. D65 (2009) 148.

[19] K. Sonogashira, Y. Tohda, N. Hagihara, Tetrahedron Lett. 16 (1975) 4467.

[20] S. Takahashi, Y. Kuroyama, K. Sonogashira, N. Hagihara, Synthesis 8 (1980) 627.

[21] R. Saravanakumar, B. Varghese, S. Sankararaman, CrystEngComm 11 (2009) 337.

[22] B. Smith, Infrared Spectral Interpretation, CRC Press, New York, 1999.

[23] F. Katzsch, D. Eißmann, E. Weber, Struct. Chem. 23 (2012) 245.

[24] F.H. Herbstein, M. Kapon, G.M. Reisner, J. Inclusion Phenom. 5 (1987) 211.

[25] C. Fischer, G. Lin, W. Seichter, E. Weber, Tetrahedron 67 (2011) 5656.

[26] D. Eißmann, F. Katzsch, E. Weber, Struct. Chem. 23 (2012) 1131.

[27] C.A. Hunter, J.K.M. Sanders, J. Am. Chem. Soc. 112 (1990) 5525.

[28] P.R. Schreiner, M. Prall, V. Lutz, Angew. Chem. Int. Ed. 42 (2003) 5757.